New particle formation and growth in biomass burning plumes: An important source of cloud condensation nuclei

Christopher J. Hennigan,[1] Daniel M. Westervelt,[1] Ilona Riipinen,[2,3]
Gabriella J. Engelhart,[1] Taehyoung Lee,[4] Jeffrey L. Collett Jr.,[4] Spyros N. Pandis,[1,5]
Peter J. Adams,[1] and Allen L. Robinson[1]

[1] Experiments were performed in an environmental chamber to characterize the effects of photo-chemical aging on biomass burning emissions. Photo-oxidation of dilute exhaust from combustion of 12 different North American fuels induced significant new particle formation that increased the particle number concentration by a factor of four (median value). The production of secondary organic aerosol caused these new particles to grow rapidly, significantly enhancing cloud condensation nuclei (CCN) concentrations. Using inputs derived from these new data, global model simulations predict that nucleation in photo-chemically aging fire plumes produces dramatically higher CCN concentrations over widespread areas of the southern hemisphere during the dry, burning season (Sept.–Oct.), improving model predictions of surface CCN concentrations. The annual indirect forcing from CCN resulting from nucleation and growth in biomass burning plumes is predicted to be -0.2 W m^{-2}, demonstrating that this effect has a significant impact on climate that has not been previously considered. **Citation:** Hennigan, C. J., D. M. Westervelt, I. Riipinen, G. J. Engelhart, T. Lee, J. L. Collett Jr., S. N. Pandis, P. J. Adams, and A. L. Robinson (2012), New particle formation and growth in biomass burning plumes: An important source of cloud condensation nuclei, *Geophys. Res. Lett.*, *39*, L09805, doi:10.1029/2012GL050930.

1. Introduction

[2] Biomass burning emits large amounts of trace gases and particles into the atmosphere, influencing climate, precipitation patterns, and aquatic and terrestrial ecosystems [*Andreae et al.*, 2004; *Crutzen and Andreae*, 1990; *Ramanathan et al.*, 2007]. Fires also contribute a significant fraction of the global cloud condensation nuclei (CCN) burden [*Pierce et al.*, 2007; *Andreae*, 2009; *Spracklen et al.*,

2011]. Some of the highest ambient CCN concentrations occur in regions heavily impacted by large-scale biomass burning, such as Amazonia and sub-Saharan Africa [*Andreae and Rosenfeld*, 2008; *Andreae*, 2009]. Fire plumes are often transported for thousands of kilometers and therefore influence air quality and climate far beyond the source region [*Anderson et al.*, 1996; *Andreae et al.*, 1988].

[3] Although biomass burning likely has a significant impact on the climate system, global model predictions of CCN concentrations from biomass burning are especially uncertain [*Spracklen et al.*, 2011], complicating the quantification of aerosol indirect effects [*Intergovernmental Panel on Climate Change (IPCC)*, 2007]. Biomass burning emission inventories used by global models are based on near-field measurements of fresh emissions but the biomass burning plume is a dynamic system in which dilution [*Robinson et al.*, 2010] and oxidation [*Hobbs et al.*, 2003; *Yokelson et al.*, 2009] rapidly transform the direct (primary) gaseous and particle emissions as the plume is transported away from the fire. These transformations alter the chemical and physical properties of the primary particle emissions [*Haywood et al.*, 2003; *Hennigan et al.*, 2011], and thus, presumably, their effects on air quality and climate. However, these transformations are not included in global models and their effects on global CCN concentrations and the aerosol indirect effects are not well understood.

[4] In this study, we performed novel experiments to investigate the effects of photo-oxidation on particle number and CCN concentrations from biomass burning. We use the new experimental results to develop inputs for a general circulation model coupled with a comprehensive aerosol microphysics model (GISS-TOMAS), which represents, to our knowledge, the first global modeling assessment of particle nucleation and growth in biomass burning plumes. The model is used to predict the effects of photo-oxidation in fire plumes on global CCN concentrations and to quantify the resulting impact on climate through the cloud albedo effect.

2. Methods

[5] To investigate the atmospheric transformations of biomass burning emissions, smog chamber experiments were conducted as part of the third Fire Lab at Missoula Experiment (FLAME-III) at the US Fire Science Laboratory in Missoula, Montana. Experimental methods have been described in detail elsewhere [*Hennigan et al.*, 2011]. Briefly, fresh (primary) gas and particle emissions from controlled laboratory burns designed to simulate open wild land fires were sampled into a 7 m^3 Teflon smog chamber.

[1] Center for Atmospheric Particle Studies, Carnegie Mellon University, Pittsburgh, Pennsylvania, USA.
[2] Department of Applied Environmental Science, Stockholm University, Stockholm, Sweden.
[3] Bert Bolin Centre for Climate Research, Stockholm University, Stockholm, Sweden.
[4] Department of Atmospheric Science, Colorado State University, Fort Collins, Colorado, USA.
[5] Department of Chemical Engineering, University of Patras, Patras, Greece.

Corresponding author: A. L. Robinson, Center for Atmospheric Particle Studies, Carnegie Mellon University, 5000 Forbes Ave., Pittsburgh, PA 15213, USA. (alr@andrew.cmu.edu)
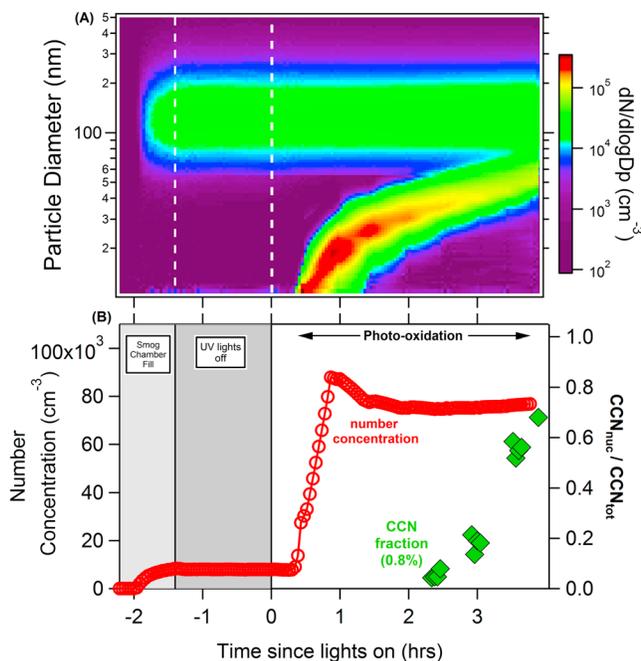
Figure 1. (a) The particle number distribution (10–500 nm), and (b) the total particle number concentration (red circles, left axis) and the fraction of CCN at 0.8% supersaturation from nucleation compared to the total CCN concentration (0.8%) (green diamonds, right axis) for an experiment with wire grass. All data have been corrected for particle losses to the chamber walls (auxiliary material).

Filling the smog chamber diluted the emissions by roughly a factor of 20 compared to concentrations in the burn chamber. After characterizing the diluted gas- and particle-phase emissions in the smog chamber for 1.4 hr, the emissions were photo-oxidized by exposing them to a combination of natural and artificial lights. Oxidant (e.g., hydroxyl radical), trace gas, and aerosol concentrations inside the chamber were comparable to typical plume conditions [*Hennigan et al.*, 2011]; therefore, the experiments investigate the transformations that occur within a few hours of the emissions entering the atmosphere. A total of 18 experiments with 12 different North American biofuels were performed under varying concentrations representative of ambient plume conditions (auxiliary material).[1]

[6] Aerosol number concentrations and size distributions were measured in the size range of 10–500 nm with a scanning mobility particle sizer (TSI - model 3080 with TSI - model 3772). Cloud condensation nuclei (CCN) measurements were made with a continuous flow streamwise thermal gradient CCN counter (DMT) and a CPC (TSI - model 3772) after preconditioning the aerosols by humidification and subsequent drying [*Engelhart et al.*, 2012]. OH levels were estimated from the measured decay of single-ring aromatic hydrocarbons with a calibrated proton-transfer-reaction mass spectrometer [*Hennigan et al.*, 2011] (Ionicon).

[7] The experimental data were implemented into a global aerosol microphysics model, Goddard Institute for Space Studies General Circulation Model II-prime (GISS-GCM-II′)

coupled to the TwO-Moment Aerosol Sectional microphysics algorithm (TOMAS). The base model setup has been described previously [*Lee and Adams*, 2010]. Additional biomass burning model inputs were derived from the experiments, and are described below. See the auxiliary material for additional model details.
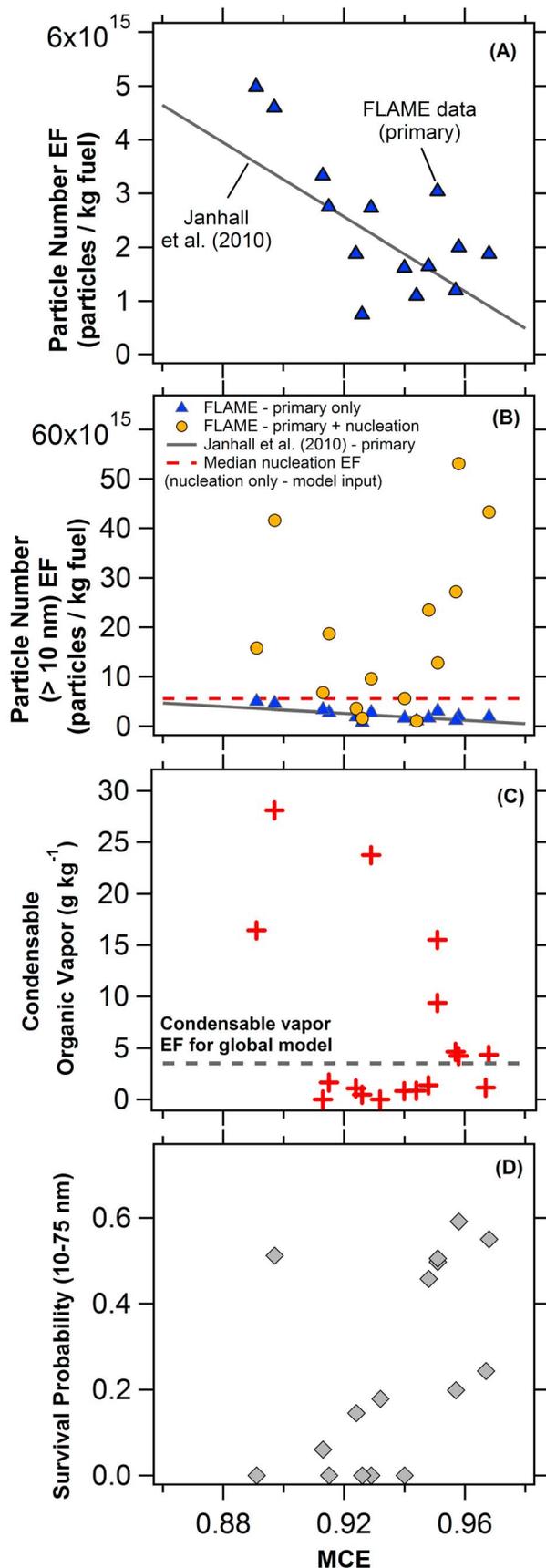
3. Results

3.1. Experimental Results

[8] Figure 1 shows time series data from a typical experiment. The primary particle emissions were dominated by accumulation mode aerosol with a number median diameter of 135 nm (Figure 1a). Exposing the chamber to UV light initiated photochemistry that created a strong nucleation burst, increasing the particle number concentration inside the chamber by a factor of 9–10 (Figures 1a and 1b). These new particles then grew at a rate of 12 nm hr^{-1} to a median size of 60 nm over the course of the 4 hr experiment (Figure 1a), demonstrating that photo-oxidation also produced significant amounts of condensable vapors. Because of this rapid growth, many of the nucleated particles survived and contributed to the measured CCN concentrations. After 3.5 hours of photo-oxidation, about 60% of the CCN at 0.8% supersaturation resulted from growth of nucleated particles (Figure 1b); the newly formed particles also activated at 0.4% supersaturation ($\sim$10% CCN$_{nuc}$/CCN$_{tot}$ ratio at 0.4% SS). Field studies have reported nucleation in both fresh (<1 hr) [*Hobbs et al.*, 2003] and aged [*Andreae et al.*, 2001] fire plumes.

[9] Figure 2 compiles nucleation and growth data from the entire set experiments. Figure 2a indicates that the primary particle number emission factors measured before photo-oxidation agree with literature data for fresh biomass burning emissions [*Janhäll et al.*, 2010]. In 17 of 18 experiments, nucleation induced by photo-oxidation greatly increased the particle number (Figure 2b). The enhancement in particle number due to nucleation was highly variable, ranging from a factor of 1.9 to 26, with a median enhancement of 3.9. Since this nucleation likely occurs shortly after the emissions enter the atmosphere (sub-grid), model parameterizations based only on primary particle emissions likely substantially underestimate the contribution of biomass burning to particle number and CCN concentrations (Figure 2b). Unlike primary particle number emissions [*Janhäll et al.*, 2010], particle number enhancements due to nucleation are not related to combustion efficiency (i.e., no correlation observed for orange symbols in Figure 2b).

[10] New particle formation was typically observed 30–60 minutes after initiating photo-oxidation, similar to the results plotted in Figure 1. Some of the delay is likely due to the lower limit of our particle size measurements (10 nm) because particle growth from clusters to 10 nm sizes is a dynamic process [*Jiang et al.*, 2011]. Finally the new particle formation occurred in the presence of a significant condensational sink (average condensational sink of the primary particles was 53.8 hr^{-1}), demonstrating that the production of condensable vapors was quite rapid.

[11] In order to become CCN, freshly nucleated particles must grow to roughly 50–100 nm, depending on supersaturation. Rapid growth was observed in every experiment; the median particle growth rate was 14 nm hr^{-1}. Sized-resolved measurements of chemical composition with an Aerosol

Mass Spectrometer indicate that this growth was due to secondary organic aerosol (SOA) formation [*Hennigan et al.*, 2011]. Particle number enhancement was also correlated with the SOA production ($R^2 = 0.61$, auxiliary material). Field studies report substantial SOA production in biomass burning plumes [*Lee et al.*, 2008; *Yokelson et al.*, 2009]. Figure 2c plots the measured mass of SOA produced relative to the amount of fuel consumed in each experiment.

[12] The rapid growth due to SOA formation resulted in a high survival probability for particle growth from 10 to 75 nm (Figure 2d) and creation of new CCN. Across all experiments, the median survival probability for particle growth from 10 to 75 nm was 18%. Even at the end of the experiment, there is clear evidence of continued particle growth (Figures 1 and S7), indicating sustained production of condensable vapors. Therefore, additional photo-oxidation is expected to result in continued growth and further increase CCN concentrations.

[13] The 10 nm particle formation rates (J_{10}) were strongly correlated with inferred H_2SO_4 concentrations ($R^2 = 0.60$), but the inferred H_2SO_4 concentrations were, on average, a factor of 20 too low to explain the observed growth rates (Figure S2). Therefore, H_2SO_4 likely plays a key role in the first steps of the formation of these particles, but their growth is dominated by SOA, in line with a number of recent field and laboratory observations [*Kuang et al.*, 2010; *Kirkby et al.*, 2011].

3.2. Modeling Results

[14] The aerosol indirect effect depends strongly on aerosol number and size [*Pierce et al.*, 2007; *Pierce and Adams*, 2009; *Spracklen et al.*, 2011], therefore nucleation and growth in fire plumes may have an important effect on global climate. To investigate this hypothesis, data obtained from this study were used as input parameters for simulations conducted with the GISS-TOMAS global aerosol microphysics model. Because nucleation occurs so quickly in our experiments (<1 hr), it was treated in the model as an enhanced emission of 10 nm particles from biomass burning.

Figure 2. Summary of results from all photo-oxidation experiments. (a) Plot of the fresh (before photo-oxidation), primary particle number emission factor (EF) measured in the smog chamber as function of modified combustion efficiency (MCE). MCE is defined as the ratio of CO_2 emitted to that of $CO + CO_2$. The primary emissions measured here agree well with the parameterization derived by *Janhäll et al.* [2010] for primary (<1–2 min) particle emissions from different biomass burning source classes. (b) Comparison of the effects of nucleation to primary particle EF. In relatively fresh biomass burning plumes (<1 hr), photo-oxidation induced nucleation greatly enhanced number concentration and is not related to the MCE. The red line in Figure 2b is the median effective particle number EF due to nucleation, which is higher than any of the observed primary particle number emission factors. (c) Plot of the measured production of secondary organic aerosol mass for each experiment from *Hennigan et al.* [2011], along with the median value used as an additional input of condensable vapors from biomass burning for the global modeling simulations. (d) The survival probability for growth from 10 to 75 nm for each experiment (auxiliary material).
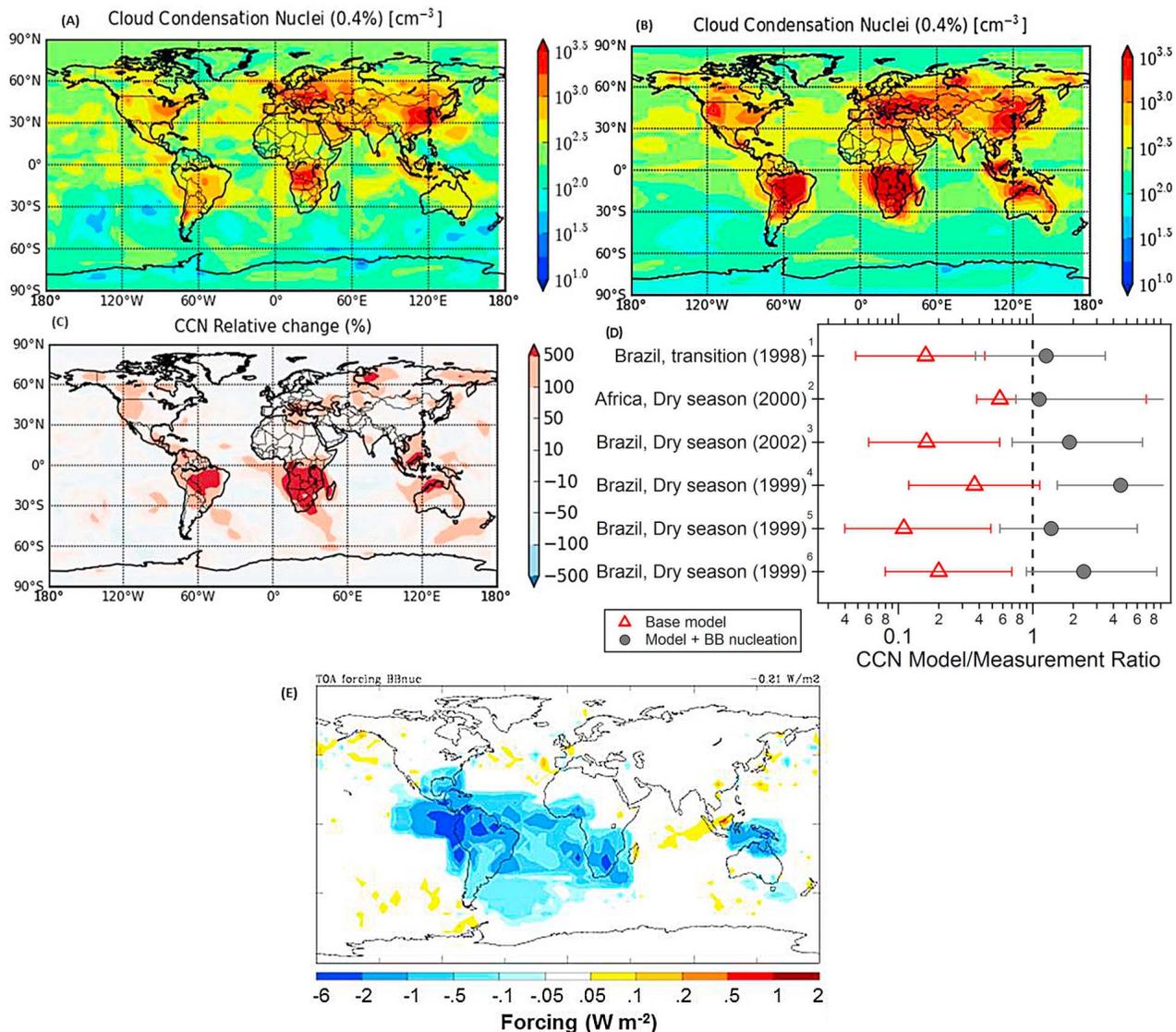
Figure 3. Predicted surface CCN concentrations (0.4% supersaturation) averaged over Sept.–Oct (burning season) for (a) base model (no biomass burning nucleation) and (b) revised model with nucleation and growth inputs derived from experiments. (c) The relative increase in CCN (0.4%) due to nucleation and growth induced by photo-oxidation in biomass burning plumes. (d) model-measurement comparisons of surface CCN concentrations. Bars represent the range and data points represent the mid-point of reported CCN concentrations (1, *Rissler et al.* [2004]; 2, *Ross et al.* [2003]; 3, *Andreae et al.* [2004]; 4, *Williams et al.* [2002]; 5, *Artaxo et al.* [2002]; 6, *Guyon et al.* [2003]). (e) Predicted annual average climate forcing (W m^{-2}) due to enhanced CCN from biomass burning nucleation and growth. This forcing considers only the effect of nucleation and growth in biomass burning plumes on cloud albedo.

The particle number emission factor was scaled using the median measured nucleation enhancement factor shown in Figure 2b. The production of condensable vapors in an oxidizing plume was defined based on the median measured SOA formation (3.51 g/kg, dashed line in Figure 2c). Additional details of the model, including these derived inputs, are available in the auxiliary material.

[15] Figures 3a and 3b show maps of predicted surface CCN concentrations (0.4% supersaturation) averaged over the dry season (September and October) when there is significant biomass burning (a similar figure for the wet season is in the auxiliary material). The revised model that accounts for nucleation and growth induced by photo-oxidation of biomass burning emissions increases predicted CCN concentrations by as much as a factor of 5 over base model simulations (Figure 3c). Consistent with observations [*Anderson et al.*, 1996; *Andreae et al.*, 1988], the predicted enhancements are spread across large geographical areas, which underscores the global influence of biomass burning emissions.

[16] To evaluate the model, predicted surface CCN concentrations are compared to measurements in Amazonia and Africa taken over the past decade [*Artaxo et al.*, 2002; *Williams et al.*, 2002; *Guyon et al.*, 2003; *Ross et al.*, 2003; *Andreae et al.*, 2004; *Rissler et al.*, 2004]. The revised model performs significantly better (average model/measurement

ratio = 2.1) than the base model (no biomass burning nucleation; average model/measurement ratio = 0.26) during the dry season (Figure 3d), suggesting that nucleation and growth of aerosols in biomass burning plumes impacted these locations. Other possible explanations for the underprediction of CCN levels by the base model include uncertainties in the model emission inventories and size distributions [*Spracklen et al.*, 2011]. However, we believe that nucleation and growth in biomass burning plumes is a significant part of the explanation since we are using high estimates for primary biomass burning emissions. Further, analogous simulations performed in GEOS-Chem also showed systematic underpredictions by the base model that are difficult to reconcile based solely on primary emissions (auxiliary material).

[17] The revised GISS-TOMAS model predicts that new particle formation and growth in fire plumes has a significant impact on climate by altering cloud albedo (first aerosol indirect effect). The predicted change in the globally averaged annual radiative forcing due to these processes is -0.2 W m^{-2} (Figure 3e), which corresponds to about 30% of the best estimate of the aerosol indirect effect from the most recent IPCC assessment [*IPCC*, 2007]. Current model treatments do not account for the dynamic particle formation and growth in biomass burning plumes and therefore do not fully capture the air quality and climate effects of this important pollution source.

[19] The Editor wishes to thank two anonymous reviewers for assisting with the evaluation of this paper.

References

Anderson, B. E., W. B. Grant, G. L. Gregory, E. V. Browell, J. E. Collins Jr., G. W. Sachse, D. R. Bagwell, C. H. Hudgins, D. R. Blake, and N. J. Blake (1996), Aerosols from biomass burning over the tropical South Atlantic region: Distributions and impacts, *J. Geophys. Res.*, 101, 24,117–24,137, doi:10.1029/96JD00717.

Andreae, M. O. (2009), Correlation between cloud condensation nuclei concentration and aerosol optical thickness in remote and polluted regions, *Atmos. Chem. Phys.*, 9, 543–556, doi:10.5194/acp-9-543-2009.

Andreae, M. O., and D. Rosenfeld (2008), Aerosol-cloud-precipitation interactions. Part 1. The nature and sources of cloud-active aerosols, *Earth Sci. Rev.*, 89, 13–41, doi:10.1016/j.earscirev.2008.03.001.

Andreae, M. O., et al. (1988), Biomass-burning emissions and associated haze layers over Amazonia, *J. Geophys. Res.*, 93, 1509–1527, doi:10.1029/JD093iD02p01509.

Andreae, M. O., et al. (2001), Transport of biomass burning smoke to the upper troposphere by deep convection in the equatorial region, *Geophys. Res. Lett.*, 28, 951–954, doi:10.1029/2000GL012391.

Andreae, M. O., et al. (2004), Smoking rain clouds over the Amazon, *Science*, 303, 1337–1342, doi:10.1126/science.1092779.

Artaxo, P., J. V. Martins, M. A. Yamasoe, A. S. Procópio, T. M. Pauliquevis, M. O. Andreae, P. Guyon, L. V. Gatti, and A. M. C. Leal (2002), Physical and chemical properties of aerosols in the wet and dry seasons in Rondônia, Amazonia, *J. Geophys. Res.*, 107(D20), 8081, doi:10.1029/2001JD000666.

Crutzen, P. J., and M. O. Andreae (1990), Biomass burning in the tropics—Impact on atmospheric chemistry and biogeochemical cycles, *Science*, 250, 1669–1678, doi:10.1126/science.250.4988.1669.

Engelhart, G. J., et al. (2012), Cloud condensation nuclei activity of fresh primary and aged biomass burning aerosol, *Atmos. Chem. Phys. Discuss.*, 12, 7521–7544, doi:10.5194/acpd-12-7521-2012.

Guyon, P., et al. (2003), Physical properties and concentration of aerosol particles over the Amazon tropical forest during background and biomass burning conditions, *Atmos. Chem. Phys.*, 3, 951–967, doi:10.5194/acp-3-951-2003.

Haywood, J. M., S. R. Osborne, P. N. Francis, A. Keil, P. Formenti, M. O. Andreae, and P. H. Kaye (2003), The mean physical and optical properties of regional haze dominated by biomass burning aerosol measured from the C-130 aircraft during SAFARI 2000, *J. Geophys. Res.*, 108(D13), 8473, doi:10.1029/2002JD002226.

Hennigan, C. J., et al. (2011), Chemical and physical transformations of organic aerosol from the photo-oxidation of open biomass burning emissions in an environmental chamber, *Atmos. Chem. Phys.*, 11, 7669–7686, doi:10.5194/acp-11-7669-2011.

Hobbs, P. V., P. Sinha, R. J. Yokelson, T. J. Christian, D. R. Blake, S. Gao, T. W. Kirchstetter, T. Novakov, and P. Pilewskie (2003), Evolution of gases and particles from a savanna fire in South Africa, *J. Geophys. Res.*, 108(D13), 8485, doi:10.1029/2002JD002352.

Intergovernmental Panel on Climate Change (IPCC) (2007), *Climate Change 2007: The Physical Science Basis. Contribution of Working Group I to the Fourth Assessment Report of the Intergovernmental Panel on Climate Change*, edited by S. Solomon et al., Cambridge Univ. Press, Cambridge, U. K.

Janhäll, S., et al. (2010), Biomass burning aerosol emissions from vegetation fires: Particle number and mass emission factors and size distributions, *Atmos. Chem. Phys.*, 10, 1427–1439, doi:10.5194/acp-10-1427-2010.

Jiang, J. K., et al. (2011), First measurements of neutral atmospheric Cluster and 1–2 nm particle number size distributions during nucleation events, *Aerosol Sci. Technol.*, 45, ii–v, doi:10.1080/02786826.2010.546817.

Kirkby, J., et al. (2011), Role of sulphuric acid, ammonia and galactic cosmic rays in atmospheric aerosol nucleation, *Nature*, 476, 429–433, doi:10.1038/nature10343.

Kuang, C., et al. (2010), An improved criterion for new particle formation in diverse atmospheric environments, *Atmos. Chem. Phys.*, 10, 8469–8480, doi:10.5194/acp-10-8469-2010.

Lee, Y. H., and P. J. Adams (2010), Evaluation of aerosol distributions in the GISS-TOMAS global aerosol microphysics model with remote sensing observations, *Atmos. Chem. Phys.*, 10, 2129–2144, doi:10.5194/acp-10-2129-2010.

Lee, S., et al. (2008), Diagnosis of aged prescribed burning plumes impacting an urban area, *Environ. Sci. Technol.*, 42, 1438–1444, doi:10.1021/es7023059.

Pierce, J. R., and P. J. Adams (2009), Uncertainty in global CCN concentrations from uncertain aerosol nucleation and primary emission rates, *Atmos. Chem. Phys.*, 9, 1339–1356, doi:10.5194/acp-9-1339-2009.

Pierce, J. R., et al. (2007), Contribution of primary carbonaceous aerosol to cloud condensation nuclei: Processes and uncertainties evaluated with a global aerosol microphysics model, *Atmos. Chem. Phys.*, 7, 5447–5466, doi:10.5194/acp-7-5447-2007.

Ramanathan, V., et al. (2007), Warming trends in Asia amplified by brown cloud solar absorption, *Nature*, 448, 575–578, doi:10.1038/nature06019.

Rissler, J., et al. (2004), Physical properties of the sub-micrometer aerosol over the Amazon rain forest during the wet-to-dry season transition – Comparison of modeled and measured CCN concentrations, *Atmos. Chem. Phys.*, 4, 2119–2143, doi:10.5194/acp-4-2119-2004.

Robinson, A. L., et al. (2010), Updating the conceptual model for fine particle mass emissions from combustion systems, *J. Air Waste Manage. Assoc.*, 60, 1204–1222, doi:10.3155/1047-3289.60.10.1204.

Ross, K. E., et al. (2003), Spatial and seasonal variations in CCN distribution and the aerosol-CCN relationship over southern Africa, *J. Geophys. Res.*, 108(D13), 8481, doi:10.1029/2002JD002384.

Spracklen, D. V., et al. (2011), Global cloud condensation nuclei influenced by carbonaceous combustion aerosol, *Atmos. Chem. Phys.*, 11, 9067–9087, doi:10.5194/acp-11-9067-2011.

Williams, E., et al. (2002), Contrasting convective regimes over the Amazon: Implications for cloud electrification, *J. Geophys. Res.*, 107(D20), 8082, doi:10.1029/2001JD000380.

Yokelson, R. J., et al. (2009), Emissions from biomass burning in the Yucatan, *Atmos. Chem. Phys.*, 9, 5785–5812, doi:10.5194/acp-9-5785-2009.